

IDENTIFICATION OF POTENTIAL INHIBITORS OF
HUMAN HEXOKINASE II FOR THE DEVELOPMENT
OF ANTI-DENGUE THERAPEUTICS

BY

SURIYEA TANBIN

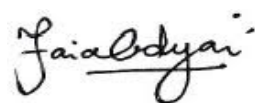
A thesis submitted in fulfillment of the requirement for the
degree of Master of Science (Biotechnology Engineering)

Kulliyyah of Engineering
International Islamic University Malaysia

MAY 2021

ABSTRACT

Dengue is one of the most common arthropod-borne viral illnesses caused by the dengue virus (DENV). Approximately, 400 million dengue infections occurred every year globally, where in Malaysia a total of 82,753 dengue cases with 133 deaths were reported until October 31, 2020. The lack of effective dengue treatment leads to an increased number of cases and deaths around the globe each year. Thus, novel anti-dengue therapies are urgently needed for effective treatment. It has been reported that a glycolytic enzyme, the human hexokinase II (HKII) has a great impact in supporting viral replication in the host cell, hence the enzyme has been proposed as a drug target. The overall aim of this work is to identify novel anti-dengue drug candidates through *in silico* screening and HKII enzymatic inhibition studies. The potential drug candidates were screened using Ultrafast Shape Recognition with CREDO Atom Types (USRCAT) program by utilizing both HKII's substrate and product; alpha-D-glucose (GLC) and beta-D-glucose-6-phosphate (BG6), as well as a known HKII's inhibitor, 2-deoxyglucose (2DG), as the query molecule. In total, selected 150 compounds with the highest similarity scores relative to three reference molecules (GLC, BG6, and 2DG) were obtained from USRCAT. The similarity scores of GLC, BG6, and 2DG analogs ranged from 0.99–0.91, 0.81–0.78, and 0.80–0.75, respectively. The selected analogs were subsequently docked against each domain of the HKII structure (PDB ID: 2NZT) using the AutoDockVina program (Version 4.2.5). The six top-ranked compounds with the best docking results for each analog were observed in the N-terminus of Chain A of HKII. The binding energy of analogs of GLC, BG6, and 2DG ranged from -7.2 to -6.7 kcal/mol, -7.8 to -7.0 kcal/mol, and -6.3 to 5.0kcal/mol, respectively. Subsequently, molecular dynamic simulations were conducted using GROMACS (Version 5), where the top two analogs for each query GLC, BG6, and 2DG were selected based on strong protein-ligand stability. Meanwhile, the recombinant HKII gene has been cloned into pET28b and pET32b vectors and successfully expressed in *Escherichia coli* BL21 (DE3) and BL21(DE3) PlySs strains at 18°C for 20 hours, with 0.5mM IPTG induction. The expressed protein was subsequently purified with a specific activity of 80. 90U.mg⁻¹ and 10.50% yield of 80 mg HKII protein by conducting a two-stage purification procedure. In the current study, the V_{max} and K_m value for HKII were determined to be 12.53uM/min, and 0.7 mM, respectively. Lastly, the inhibition analysis was conducted at different concentrations where chitin (the analog of 2DG) and 3,4-dihydroxy-5-(hydroxymethyl) (the analog of BG6) have shown a significant inhibitory effect on HKII with 36.32% and 29.58% inhibition respectively at 2mM concentration. In conclusion, among the selected compounds, chitin, which is the analog of 2DG has shown the highest inhibitory effect on human HKII, which has paved the path towards the development of future anti-dengue therapeutics.



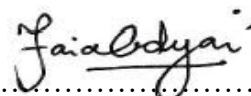
خلاصة البحث

يؤدي عدم (DENV) عدوى حمى الضنك من أكثر الأمراض المميتة في العالم ، والتي يسببها فيروس حمى الضنك وجود علاج فعال لحمى الضنك إلى زيادة عدد الوفيات على مستوى العالم كل عام .وبالتالي ، فإن العلاجات الجديدة المضادة لحمى الضنك مطلوبة للعلاج الفعال .تم اختيار الأدوية المرشحة المحتملة باستخدام الفحص القائم على الترابط في المجموع 150 مركبًا بأعلى HKII أخيرًا ، تم إجراء دراسة حركية الإنزيم ودراسة التثبيت باستخدام مقايسة تثبيط من خلال الفحص المستند إلى α -D-glucose (GLC) و β -D-glucose-6-phosphate (BG6) و 2-deoxyglucose (2-DG) من خلال الفحص القائم على الهيكلي . في المجموع ، تم إدراج 18 مركبًا كأفضل مثبط ligand وتم الشروع في إجراء مزيد من الفحص القائم على الهيكلي . تراوحت درجات التشابه بين نظائرها والجزيئات من 0.91 - 0.99 و 0.78 - 0.81 و 0.75 - 0.80 لجزيئات DG و BG6 و GLC من باستخدام (PDB: 2NZT معرف) HKII الاستعلام الثلاثة ، على التوالي . تم ربط نظائرها لاحقًا بالبنية البلورية حيث توجد المواقع النشطة والروابط القوية . تتمتع ضربات ، B و A في السلسلة Auto Dock Vina برنامج بأفضل طاقة ربط تتراوح من -7.2 إلى -6.7 ، DG و BG6 و GLC الالتحام ، وهي جزيئات مشابهة لكيلو كالوري /مول ، و -7.8 إلى -7.0 كيلو كالوري /مول و -6.3 إلى -5.0 كيلو كالوري /مول ، على طرف على التوالي . علاوة على ذلك ، تم اختيار إجمالي 6 مركبات غير سامة مع أفضل وضع للرسو لمحاكاة A N السلسلة DG و BG6 و GLC ، حيث أظهر المركب 1 و 3 ، المركب 8 و 9 ، المركب 13 و 14 ، النظير من MD المؤتلف بنجاح في نواقل HKII على التوالي استقرارًا قويًا ليجند البروتين . من ناحية أخرى ، تم استنساخ جين TB أفضل تعبير في وسائط BL21 (DE3) في pET28b-HKII وأظهر بناء pET32b و pET28b HKII أخيرًا ، تم الحصول على IPTG (مرق رائع (عند 18 درجة مئوية لمدة 20 ساعة مع 0.5 ملي مولار ، $U.mg^{-1}$ مع نشاط محدد 80.90 HKII النقي من مزرعة 2 لتر مع إنتاجية 10.5 % من بروتين 80 مجم وكانت المرحلة النهائية هي تحليل تثبيط نظائرها المختارة وتم إجراء تحليل تثبيط لنظائرها المختارة عند ثلاثة تراكيز مختلفة $3,4\text{-}(2S, 3R, 4S, 5S)\text{-BG6}$ ؛ 36.62% ؛ بينما نظائرها من DG مم ، 5 مم و نظائر 2 2 $4,5\text{-dihydro-1H-purin-6-yl}\text{-}(5\text{-hydroxymethyl})\text{-tetrahydrofuran-2-yl}$ -3،4-dihydroxy-5- (hydroxymethyl) tetrahydrofuran-2-yl] -4،5-dihydro-1H-purin-6 (مجموع 9 ؛ 29.58% تثبيط عند 10 ملي مول ، وفي الختام ، فإن المركبات المختارة من الفحص 6 purin-6 البشري ، والتي يمكن تطويرها بشكل أكبر كعلاجات HKII الافتراضي لديها إمكانية كبيرة لإظهار تأثير التثبيت على مستقبلية لمكافحة حمى الضنك .

Dr. Nassereldeen Ahmed Kabbashi

APPROVAL PAGE

I certify that I have supervised and read this study and that in my opinion, it conforms to acceptable standards of scholarly presentation and is fully adequate, in scope and quality, as a thesis for the degree of Master of Science (Biotechnology Engineering



.....
Fazia Adyani Ahmad Fuad
Supervisor

.....
Azzmer Azzar Abdul Hamid
Co-Supervisor

I certify that I have read this study and that in my opinion, it conforms to acceptable standards of scholarly presentation and is fully adequate, in scope and quality, as a thesis for the degree of Master of Science (Biotechnology Engineering).

.....
Yumi Zuhanis Has-Yun Hashim
Internal Examiner

.....
Mervyn Liew Wing On
External Examiner

This thesis was submitted to the Department of Biotechnology Engineering and accepted as a fulfillment of the requirement for the degree of Master of Science (Biotechnology Engineering)

.....
Nor Fadhillah Mohamed Azmin
Head, Department of
Biotechnology Engineering

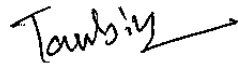
This thesis was submitted to the Kulliyah of Engineering and is accepted as a fulfillment of the requirement for the degree of Master of Science (Biotechnology Engineering)

.....
Sany Izan Ihsan
Dean, Kulliyah of Engineering

DECLARATION

I hereby declare that this thesis is the result of my own investigations, except where otherwise stated. I also declare that it has not been previously or concurrently submitted as a whole for any other degrees at IIUM or other institutions.

Suriyea Tanbin



Signature

Date18/05/2021.....

INTERNATIONAL ISLAMIC UNIVERSITY MALAYSIA

**DECLARATION OF COPYRIGHT AND AFFIRMATION OF
FAIR USE OF UNPUBLISHED RESEARCH**

**IDENTIFICATION OF POTENTIAL INHIBITORS OF HUMAN
HEXOKINASE II FOR THE DEVELOPMENT OF ANTI-
DENGUE THERAPEUTICS**

I declare that the copyright holders of this thesis are jointly owned by the student and IIUM.

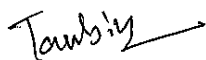
Copyright © 2021 Suriyea Tanbin and International Islamic University Malaysia. All rights reserved.

No part of this unpublished research may be reproduced, stored in a retrieval system, or transmitted, in any form or by any means, electronic, mechanical, photocopying, recording, or otherwise without prior written permission of the copyright holder except as provided below

1. Any material contained in or derived from this unpublished research may be used by others in their writing with due acknowledgment.
2. IIUM or its library will have the right to make and transmit copies (print or electronic) for institutional and academic purposes.
3. The IIUM library will have the right to make, store in a retrieved system and supply copies of this unpublished research if requested by other universities and research libraries.

By signing this form, I acknowledged that I have read and understood the IIUM Intellectual Property Right and Commercialization policy.

Affirmed by Suriyea Tanbin



.....

Signature

19/05/2021

.....

Date

ACKNOWLEDGEMENTS

In the name of Allah, The most gracious and the most merciful

Firstly, my gratitude goes to Allah swt. for His blessing in sustenance and the best of health. I am thankful that I can finish this study on time regardless of the obstacles that I face throughout the course to finish this program.

I wish to express my appreciation and special thanks to my main supervisor Assistant Prof. Dr. Fazia Adyani Ahmad Fuad, co-supervisor Assistant Prof. Dr. Azzmer Azzar Abdul Hamid, and Dr. Anuar bin jonet for believing in me to conduct the research. This journey would have been tougher if it was without their continuous guidance. Both of them are truly supportive and the knowledge, idea, and opinions shared are highly appreciated.

Next, I would like to take this opportunity to deliver my gratitude to my family especially my mother, Farida Begum, and my father, Salim Shaikh for their blessing and continuous prayer. Special thanks to my brother Faisal Shaikh and my fiancé, Md Imran Hossain for supporting and helping me a lot, as well as my uncle Amin Jooma for always taking care of me.

Finally, I want to thank the Department of Biotechnology Engineering, Kulliyah of Engineering, IIUM (Gombak), the Department of Biotechnology, Kulliyah of Science, IIUM (Kuantan), and Malaysian Genome Institute (MGI) for the opportunity given, especially to be involved in this research. The facilities in the laboratories have helped me a lot in completing these studies. My cordial thanks to the Ministry of Higher Education Malaysia. This work was supported by Fundamental Research Grant Scheme (FRGS/1/2016/STG04/UIAM/02/1), Ministry of Higher Education Malaysia (MOHE).

TABLE OF CONTENTS

Abstract	i
Abstract in Arabic	ii
Approval Page.....	iii
Declaration.....	iv
Copyright Page.....	v
Acknowledgements.....	vi
Table of Contents	vii
List of Tables	x
List of Figures	xii
List of Abbreviations	xix
List of Symbols	xx
CHAPTER ONE: INTRODUCTION	1
1.1 Background of the Study	1
1.2 Statement of the Problem	4
1.3 Research Objectives	5
1.4 Research Methodology	6
1.5 Research Scope.....	6
1.6 Thesis Organization.....	8
CHAPTER TWO: LITERATURE REVIEW.....	10
2.1 Introduction	10
2.2 Overview on the History of Dengue.....	10
2.2.1 Etymology of Dengue.....	10
2.2.2 History of Epidemiology	11
2.2.3 Dengue in Malaysia.....	14
2.3 Dengue Virus (DENV)	16
2.3.1 Taxonomy and Evolution	16
2.3.2 Serotypes of DENV	17
2.3.3 Structure of DENV	17
2.3.3.1 Structural Protein	20
2.3.3.2 Non-Structural Protein.....	20
2.4 Transmission and Replication of Dengue Virus.....	22
2.4.1 Transmission of DENV	22
2.4.2 Replication of DENV	23
2.4.2.1 Viral Attachment-Entry-Fusion	24
2.4.2.2 Viral RNA Translation and Replication	24
2.4.2.3 Maturation and Release of Viral Particles	24
2.5 Symptoms of Dengue Diseases	25
2.6 Prevension of Dengue.....	27
2.6.1 Dengue Vaccines	27
2.6.2 Licensed Vaccine and Controversy	30
2.6.3 Challenges of Dengue Vaccine Development.....	30
2.7 Drug Development Against Dengue Virus (DENV).....	31
2.7.1 Viral-Drug Targets and Inhibitors	31

2.7.2 Host-Drug Targets and Inhibitors.....	35
2.8 Significance of Host Glycolytic Pathway on DENV Survival.....	41
2.9 Glycolysis is Activated by Human Hexokinase II During dengue Infection ..	44
2.10 Human hexokinase II (HKII) As an Anti-Dengue Drug Target.....	46
2.11 Current Dengue Drug	51
2.12 Challenges of Dengue Drug Development.....	52
2.13 Strategy of Drug Development.....	52
2.13.1 High-Throughput Screening.....	53
2.13.2 Virtual-Screening.....	53
2.14 Summary.....	57
CHAPTER THREE: MATERIALS AND METHODS	58
3.1 Introduction	58
3.2 Materials	61
3.3 Methods	63
3.3.1 Ligand-Based Screening.....	64
3.3.1.1 Identification of Lead Molecules and Analogues.....	64
3.3.1.2 ADME test.....	65
3.3.1.3 Toxicity Test.....	66
3.3.2 Structure-Based Screening	66
3.3.2.1 Structural Protein Preparation.....	66
3.3.2.2 Ligand Preparation.....	67
3.3.2.3 Molecular Docking Using Auto Dock Vina	68
3.3.3 Molecular Docking Simulation	70
3.3.3.1 HKII Protein Preparation in GROMACS Format	71
3.3.3.2 Preparation of Ligand's Topology Files	72
3.3.3.3 Setup the Simulation Box	73
3.3.3.4 Running the Production of Simulation	73
3.4 Molecular Cloning	74
3.4.1 Plasmid DNA Isolation.....	74
3.4.2 Digestion with Restriction Enzyme.....	74
3.4.3 Ligation and Transformation of DNA Fragments	75
3.4.4 Colony PCR.....	76
3.4.5 Initial Culture and HKII Protein Expression	77
3.4.6 Dot-Blot Analysis	79
3.4.7 SDS-PAGE Analysis	79
3.4.8 Purification of HKII Protein	80
3.4.8.1 Large Scale Protein Expression and Cell Lysis.....	80
3.4.8.2 Immobilised Metal Ion Affinity Chromatography (IMAC) ...	81
3.4.8.3 Size Exclusion Chromatography (SEC)	81
3.4.9 Hexokinase II Activity Assay.....	82
3.4.10 Kinetics Study of Bacterially-Expressed HKII	83
3.4.11 HKII Inhibition Assay	84
CHAPTER FOUR : RESULTS AND DISCUSSION	86
4.1 Introduction	86
4.2 Virtual Screening	87
4.2.1 Ligand-Based Screening.....	87
4.2.1.1 ADME Analysis.....	96

4.2.2 Structure-Based Screening	102
4.2.2.1 Identification of Protein Binding Site.....	103
4.2.2.2 Molecular Docking for Compound from USRCAT	108
4.2.3 Toxicity Test Result	127
4.2.4 Molecular Dynamics Simulation of Selected Protein-Ligand.....	133
4.2.4.1 Analysis of Protein-Ligand Stability	133
4.2.4.2 Analysis of Hydrogen Bonds.....	142
4.3 Cloning, Expression and Purification of Human HKII	151
4.3.1 Construction of Recombination pET28b-HKII and pET32b-HKII.....	151
4.3.2 Expression of Recombinant HKII in <i>E.coli</i>	157
4.3.2.1 Dot-Blot Analysis	161
4.3.3 Purification Step for Recombinant Human HKII Protein	164
4.3.3.1 Initial Step: Metal-Affinity Chromatography (IMAC).....	164
4.3.3.2 Polishing Step: Size-Exclusion Chromatography (SEC).....	166
4.4 Human Hxokinase II Enzyme Assay	168
4.4.1 Determination of Protein Concentration	168
4.4.2 Human HKII Enzyme Assay and Kinetics	169
4.4.3 Inhibition Analysis of Bacterially-Expressed Human HKII.....	176
4.5 Summary.....	234
CHAPTER FIVE: CONCLUSION AND RECOMMENDATION.....	235
5.1 Introduction	235
5.2 Recommendation	237
REFERENCES.....	239
APPENDICES	263
APPENDIX A: Virtual-Screening Work	263
APPENDIX B: Experimental Work	266
APPENDIX C: Calculation of Experimental Work.....	271
APPENDIX D: Publications and Conferences	273

LIST OF TABLES

Table 2.1	Structural and functional properties of dengue virus protein	23
Table 2.2	Dengue vaccine candidates in clinical trials	29
Table 2.3	Anti-dengue inhibitors against viral protein	34
Table 2.4	Anti-dengue inhibitors against the host target protein	39
Table 2.5	Current anti-dengue drug on clinical trials	51
Table 3.1	List of soft wares and device	61
Table 3.2	List of Chemicals and equipment	62
Table 3.3	The Measurement of the three-dimensional grid box	70
Table 3.4	The composition of the digestion reaction	74
Table 3.5	The composition of the ligation reaction	75
Table 3.6	Primers used for the expression construction	77
Table 3.7	The parameters of expression trials	78
Table 4.1	Similarity scores and Lipinski's values for GLC and its analogs, as obtained from USRCAT	91
Table 4.2	Similarity scores and Lipinski's values for BG6 and its analogs, as obtained from USRCAT	92
Table 4.3	Similarity scores and Lipinski's values for 2DG and its analogs, as obtained from USRCAT	93
Table 4.4	The ADME analysis of GLC and its analogs	97
Table 4.5	The ADME analysis of BG6 and its analogs	98
Table 4.6	The ADME analysis of 2DG and its analogs	99
Table 4.7	The top six compound analogs of GLC are ranked according to their binding energy	111
Table 4.8	The top six compound analogs of BG6 are ranked according to their binding energy	112

Table 4.9	The top six compound analogs of 2DG are ranked according to their binding energy	113
Table 4.10	Toxicity value of GLC and analogs	130
Table 4.11	Toxicity value of BG6 and analogs	131
Table 4.12	Toxicity value of 2DG and analogs	132
Table 4.13	Expression condition of human HKII protein	158
Table 4.14	The optimized expression conditions for human HKII	159
Table 4.15	The concentration of HKII protein	169
Table 4.16	The purification table for Recombinant human HKII protein	172
Table 4.17	Comparison of kinetics parameters of HKII using different plot	174
Table 4.18	Kinetics properties (<i>K_m</i> and <i>V_{max}</i>) of HKII from different sources	176
Table 4.19	The list of compounds for inhibition analysis	178
Table 4.20	Inhibition analysis of selected compound at 2mM, 5mM, and 10mM concentration.	185

LIST OF FIGURES

Figure 1.1	The flow chart of research activities proposed in this study	7
Figure 2.1	The world distribution of dengue disease and its vector; <i>Aedes Aegypti</i>	13
Figure 2.2	Number of dengue cases from 1980 to 2017	14
Figure 2.3	Number of Dengue Cases and Deaths for Malaysia	16
Figure 2.4	Number of dengue cases reported weekly in 2019 and 2020	16
Figure 2.5	The general structure of dengue virus with the schematic representation of mature virion Envelop Protein (E), Capsid protein (C), and Membrane protein (M).	19
Figure 2.6	Dengue viral genome	20
Figure 2.7	The sylvatic and endemic urban cycle of dengue transmission	24
Figure 2.8	The schematic representation of dengue virus replication inside the human body	26
Figure 2.9	Host glycolytic pathways are necessary for dengue replication. Dengue required fatty acids for replication and virion envelopment, resulting in virus-mediated modifications in the host cellular system.	43
Figure 2.10A	Glucose is necessary for dengue virus production. HFFs were infected with DENV at an MOI of 3 and fed replete, glucose-free, or glutamine-free medium at 3 hpi.	45
Figure 2.10B	Glucose uptake is increased during DENV infection. At 24 hpi, mock- and DENV-infected (MOI of 9) HFFs were exposed to a radiolabelled glucose analog for 5 min and then intracellular radioactivity was quantified.	45
Figure 2.10C	Expression levels of HK2 are elevated in DENV-infected cells	45
Figure 2.11	The catalytic reaction of human hexokinase.	46
Figure 2.12	The crystal structure of human HKII (PDB ID:2NZT). Blue and Red represent chain A and chain B respectively. Each chain	47

	contains Alpha-D-Glucose (GLC) cyan color and Beta-D-glucose-6-phosphate (BG6) yellow color.	
Figure 2.13	The glycolytic pathway of human cell. The drug target (HKII) is indicated in the blue color	50
Figure 2.14	The steps involved in high-throughput and virtual screening	56
Figure 3.1	Flow chart	60
Figure 3.2	The 3D structure of the query molecule (GLC, BG6, and 2DG) which were used for USRCAT.	65
Figure 3.3	Native crystal structure of human HKII retrieves from protein data bank (PDB ID: 2NZZ).	69
Figure 3.4	General workflow of MD simulation	71
Figure 4.1	The 3D structure of the top six compounds with the highest similarity scores	94
Figure 4.2	Workflow of structure-based screening (SBVS)	103
Figure 4.3A	The native structure of human hexokinase II in complex with GLC (red) and BG6 (blue) in ribbon form (PDB ID: 2NZZ), retrieved from the PDB database.	105
Figure 4.3B	The N terminal domain of HKII is complex with GLC (red) and BG6 (blue), which are substrate and product, respectively. The black circle indicates the catalytic cleft of HKII, where known ligands (GLC, BG6, and 2DG) was docked.	105
Figure 4.3C	GLC, BG6, and 2DG were docked into the catalytic site. The surface representation of HKII	105
Figure 4.4A	GLC complex with HKII, where the catalytic residues involved are Thr172, Lys173, Asn208, Asn235, Asp209, and Glu260.	107
Figure 4.4B	BG6 in complex with HKII, where the catalytic residues are Ser415, Asp84, Asn89, Thr232, Lys173, Gly231, and Gln291.	107
Figure 4.4C	2DG in complex with HKII, where the catalytic residues are Ser234, Asn235, Asp209, Asn208, Lys173, Gln291, Glu294.	107
Figure 4.5	(A) GLC docked with HKII; Showing H bond Asn235, Glu260, Asp209, and Lys173. (B) compound 1 docked with HKII; showing H bond Asn208, Asp209, Lys173, Gln291 while cyan color indicates halogen bond with Ser155, Phe156, and Glu260. (C) compound 2 docked with HKII; showing H bonds Gly87,	115

- Asn89, Asp84, and Ser449 while cyan and gray color indicate carbon H bond and halogen bond with respectively. (D) compound 3 docked with HKII; showing H bond with Ser449, Thr88, Arg91 while orange color bonds indicate salt bridge with Asp84 and Asp413. 2D interaction of all complex analysis has shown at the right site and 3D interaction analysis has shown on the left side.
- Figure 4.6 BG6 docked with HKII; Showing H bond Asp209, Asn208, Gln291, Gly87, Pro157, Asp209, and Lys173. (B) Compound 7 docked with HKII; showing H bond Asp84, Asp209, Arg91, Thr232, Asn89, Thr88 while cyan color indicates halogen bond with Gly87. (C) Compound 8 docked with HKII; showing H bonds Asp84, Asn89, Thr88, Thr232, and Ser415 (D) Compound 9 docked in complex with HKII; showing H bond with Ser449, Thr88, Asn89. 2D interaction of all complex analysis shown at the right site and 3D interaction analysis shown at left side. 118
- Figure 4.7 2DG docked with HKII; Showing H bond Gly233, Lys173, Ser155, Glu294, Thr172, Asn208, Asp209 Glu260, Phe156, and Ile229. (B) Compound 13 docked with HKII; showing H bond Ser449, Asp84, Arg91 Asp84, Asp209, and Asp413 while orange color indicates salt bridge bond with Asp209, Asp84, and Asp413. (C) Compound 14 docked with HKII; showing H bonds Gly414, Gly87, Thr232, Ile229, Asp84, Asp413 (D) Compound 15 docked with HKII; showing H bond with Thr232, Thr88, Asp431, Asp84, Asp209, and Gly87. 2D interaction of all complex analysis shown at the right site and 3D interaction analysis shown at left side. 122
- Figure 4.8 (A) The imposed RMSD of the complex HKII-GLC (blue), HKII-Comp1(red), HKII-comp2(green), and HKII-comp3(black) complex have shown during 20 ns of MD simulation. (B) The imposed RMSF of the HKII-GLC (blue), HKII-comp1(red), HKII-comp2 (green), and HKII-comp3 (black) complexes generated during the trajectory period of 20 ns MD simulation. (C) Snapshot superimpose of trajectory structure of HKII-GLC, HKII-comp1, and HKII-comp2 at 10ns (yellow) and 20ns (red) MD simulation. Protein presented as cyan-colored ribbon format 136
- Figure 4.9 (A) The imposed RMSD of the complex HKII-BG6 (blue), HKII-Comp7(red), HKII-comp8(green), and HKII-comp9(black) complex have shown during 20 ns of MD simulation. (B) The imposed RMSF of the HKII-BG6 (blue), HKII-comp7(red), HKII-comp8 (green), and HKII-comp9 (black) complexes generated during the trajectory period of 20 ns MD simulation. (C) Snapshot superimpose of trajectory 138

structure of HKII-BG6, HKII-comp8, and HKII-comp9 at 10ns (blue) and 20ns (red) MD simulation. Protein presented as cyan-colored ribbon format

- Figure 4.10 (A) The imposed RMSD of the complex HKII-2DG (blue), HKII-Comp13(red), HKII-comp14(green), and HKII-comp15(black) complex have shown during 20 ns of MD simulation. (B) The imposed RMSF of the HKII-2DG (blue), HKII-comp13(red), HKII-comp14 (green), and HKII-comp15 (black) complexes generated during the trajectory period of 20 ns MD simulation. (C) Snapshot superimpose of trajectory structure of HKII-2DG, HKII-comp13, and HKII-comp14 at 10ns (blue) and 20ns (red) MD simulation. Protein presented as cyan-colored ribbon format 141
- Figure 4.11 (A) Total number of hydrogen bond interactions between HKII and comp1(red), comp2(green), comp3(black), and reference molecule GLC (blue). (B) Minimum distance analysis between HKII and comp1(red), comp2(green), comp3(black), and GLC (blue). (C) Snapshots of complex HKII-comp1 and HKII-comp3 were extracted from the trajectory at 20ns. HKII-comp1 has shown six H bonds; four formed with Lys173 and Asp209, two formed with Asn208 and Gln291. HKII-com3 has shown six H bonds three formed with Thr88, one H bond with Asp84, and two bonds formed with Asp413 and Ser449. The distance between HKII and comp1 (yellow), comp3(cyan) are average 2.03Å and 1.02Å respectively. 144
- Figure 4.12 (A) Total number of hydrogen bond interactions between HKII and comp1(red), comp2(green), comp3(black), and reference molecule GLC (blue). (B) Minimum distance analysis between HKII and comp1(red), comp2(green), comp3(black), and GLC (blue). (C) Snapshots of complex HKII-comp1 and HKII-comp3 were extracted from the trajectory at 20ns. HKII-comp1 has shown six H bonds; four formed with Lys173 and Asp209, two formed with Asn208 and Gln291. HKII-com3 has shown six H bonds three formed with Thr88, one H bond with Asp84, and two bonds formed with Asp413 and Ser449. The distance between HKII and comp1 (yellow), comp3(cyan) are average 2.03Å and 1.02Å respectively. 146
- Figure 4.13 (A) Total number of hydrogen bond interactions between HKII and comp13 (red), comp14(green), comp15(black), and reference molecule 2DG (blue). (B) Minimum distance analysis between HKII and comp13(red), comp14(green), comp15(black), and 2DG (blue). (C) Snapshots of complex HKII-comp13 and HKII-comp14 were extracted from the trajectory at 20ns. HKII-comp13 has shown seven H bonds; three formed with Asp209, four formed with Ser449, Asp84, 149

and Asp413. HKII-com14 has shown three H bonds; three formed with Asp413, Asp84, and Asp209. The distance between HKII and comp13 (yellow), comp14(cyan) are average 2.01 and 1.09 respectively.

- Figure 4.14 Agarose electrophoresis (0.8% (W/V)) of the PCR amplified HKII from pETiteN-His SUMO vector. Well, 1 to 4 depicts the template DNA (HKII) bands with 2.7kb (indicated with black arrow). M is Promega 1 kb DNA Ladder 152
- Figure 4.15 Agarose electrophoresis (0.8% (w/v)) of the digested vectors and PCR amplified HKII with *Bam*HI and *Hind*III. (A) Digested pET28b vector size with 5.3kb (well 1 and 2) and pET32b vector size with 5.9kb (well 3 and 4). (B) Digested PCR amplifies HKII size with 2.7kb (well 5 and 6). M is Promega 1 kb DNA Ladder. 149 153
- Figure 4.16 Verifications of the transformants by colony PCR. PCR was performed on seven transformed colonies and four were shown to contain HKII insert. Well, 1,4,5, and 7 showing the HKII band size with 2.7kb. 153
- Figure 4.17 Verification of transformants by restriction enzymes analysis. Well, 1 and 2 indicate the double digestion of construct pET28b-HKII with *Bam*HI and *Hind*III; pET28b size 5.3kb and HKII size 2.7kb. Well, 3 and 4 indicate the double digestion of construct pET32b-HKII with *Bam*HI and *Hind*III; pET32b size 5.9kb and HKII size 2.7kb. 154
- Figure 4.18 (A) Verification of transformant by DNA sequencing. Alignment between HKII gene reference sequence and sequencing result. Query: sequencing result. Subject: reference sequence. (B) The plasmid map of the constructed His. tagged HKII (pET28b-HKII and pET32b-HKII). 156
- Figure 4.19 Human HKII expression trials in TB media at 18°C for 20 hours in. A 10% SDS-PAGE is shown with 2-4µg samples of IPTG (0.5mM)-induced samples containing HKII. (A) Lanes (1 to 4) are soluble fractions of all samples; lanes 1 (pET28b-HKII in BL21(DE3)) and lanes 2 (pET28b-HKII in BL21(DE3) PlySs), lanes 3 (pET32b-HKII in BL21(DE3)), lanes 4 (pET32b-HKII in BL21(DE3) PlySs). (B) Lanes (5 to 8) are an insoluble fraction of all samples; lanes 5 (pET28b-HKII in BL21(DE3)) and lanes 6 (pET28b-HKII in BL21(DE3) PlySs), lanes 7 (pET32b-HKII in BL21(DE3)), lanes 8 (pET32b-HKII in BL21(DE3) PlySs). C indicates the non-induced IPTG sample. M indicates pre-strain protein marker. The red arrow indicates the expressed HKII protein band (102kDa). 160

- Figure 4.20 Human HKII expression trials in LB media at 18°C for 20 hours in. A 10% SDS-PAGE is shown with 2-4µg samples of IPTG (0.5mM)-induced samples containing HKII. (A) Lanes (1 to 4) are soluble fractions of all samples; lanes 1 (pET28b-HKII in BL21(DE3)) and lanes 2 (pET28b-HKII in BL21(DE3) PlySs), lanes 3 (pET32b-HKII in BL21(DE3)), lanes 4 (pET32b-HKII in BL21(DE3) PlySs). (B) Lanes (5 to 8) are an insoluble fraction of all samples; lanes 5 (pET28b-HKII in BL21(DE3)) and lanes 6 (pET28b-HKII in BL21(DE3) PlySs), lanes 7 (pET32b-HKII in BL21(DE3)), lanes 8 (pET32b-HKII in BL21(DE3) PlySs). C indicates the non-induced IPTG sample. M indicates pre-strain protein marker. The red arrow indicates the expressed HKII protein band (102kDa). 161
- Figure 4.21 Dot Blot analysis of Human HKII onto Polyvinylidene Fluoride (PVDF) membrane in TB media at 18°C for 20 hours in. Each dot involves spotting 1-2µl of all samples. Dots 1, 2, and 5,6 have shown a soluble fraction of construct pET28b-HKII and pET32b-HKII in BL21(DE3) and BL21(DE3) PlySs respectively where dots 3,4 and 7,8 have shown an insoluble fraction of construct pET28b-HKII and pET32b-HKII in BL21(DE3) and BL21(DE3) PlySs respectively. 162
- Figure 4.22 Dot Blot analysis of Human HKII onto Polyvinylidene Fluoride (PVDF) membrane in LB media at 18°C for 20 hours in. Each dot involves spotting 1-2µl of all samples. Dots 1, 2, and 5,6 have shown a soluble fraction of construct pET28b-HKII and pET32b-HKII in BL21(DE3) and BL21(DE3) PlySs respectively where dots 3,4 and 7,8 have shown an insoluble fraction of construct pET28b-HKII and pET32b-HKII in BL21(DE3) and BL21(DE3) PlySs respectively 162
- Figure 4.23 The elution profile of human HKII from IMAC column (A) chromatographic profile of the recombinant HKII protein where the peak indicates the eluted fraction containing HKII. (B) The eluted fraction contains HKII protein only which produces one peak distinguishable between fractions between 25 to 35ml. (C) well, 1 to 5 indicate purified HKII protein on 10% SDS-PAGE. C indicates crude sample as a control, black arrow indicates the purified HKII band (102KDa) and M labeled as a protein marker. 166
- Figure 4.24 The elution profile of human HKII from SEC column (A) chromatographic profile of the recombinant HKII protein by size exclusion chromatography (SEC). The circle indicates the HKII containing fraction (B) The eluted fraction contain HKII protein only which produces one peak distinguishable between fraction between 11 to 16ml. (C) Well, 1 to 6 indicates purified 167

HKII protein on 10% SDS-PAGE. The black arrow indicates the purified HKII band (102KDa).

Figure 4.25	The scheme represents the reaction of human HKII where glucose is converted to glucose-6-phosphates. G6P converts to 6-phosphogluconolactone by glucose -6-phosphate dehydrogenase and produces NADPH (co-factor).	169
Figure 4.26	Effect of incubation time on the reaction rate of recombinant human HKII.	172
Figure 4.27	(A) Michaelis Menten Plot for HKII with glucose as substrate (B) Lineweaver and Burk Plot for HKII with glucose as substrate.	174
Figure 4.28	Inhibition analysis of all queries (GLC, BG6, and 2DG) and their analogs at 2mM concentration. The negative control is without any inhibitor. (A) Percentage of Inhibition and remaining activity of selected compounds.	180
Figure 4.29	Inhibition analysis of all queries (GLC, BG6, and 2DG) and their analogs at 5mM concentration. The negative control is without any inhibitor. (A) Percentage of Inhibition and remaining activity of selected compounds	182
Figure 4.30	Inhibition analysis of all queries (GLC, BG6, and 2DG) and their analogs at 5mM concentration. The negative control is without any inhibitor. (A) Percentage of Inhibition and remaining activity of selected compounds	184

LIST OF ABBREVIATIONS

DENV	Dengue virus
DF	Dengue fever
DHF	Dengue hemorrhagic fever
DSS	Dengue shock syndrome
CYD-TDV	Chimeric yellow fever virus–DENV tetravalent dengue vaccine
RBC	Red blood cell
HKII	Human hexokinase II
MD	Molecular dynamics simulation
PDB	Protein data bank
HTS	High-throughput screening
GLC	Alpha-D-Glucose
BG6	Beta-D-glucos-6-phosphate
2DG	2-deoxyglucose
IMAC	Immobilized Metal Ion Affinity Chromatography
SEC	Size exclusion chromatography chromatography
ADME	Absorption, distribution, metabolism, and excretion
VMD	Visual Molecular Dynamics
ATB	Automated force field Topology Builder
TB	Terrific broth
RNA	Ribonucleic acid
cDNA	Complementary DNA
LB	Luria-Bertani broth
NADPH	Nicotinamide adenine dinucleotide phosphate hydrogen
PDBQT	Protein Data Bank, Partial Charge (Q), & Atom Type (T)
TDV	Tetravalent dengue vaccine
MgCl ₂	Magnesium Chloride Hexahydrate
NaCl	Sodium chloride
SDS-PAGE	Sodium dodecyl sulphate–polyacrylamide gel electrophoresis
TCA	Tricarboxylic acid
G-6PDH	Glucose-6-Phosphate Dehydrogenase
HFFs	Human foreskin fibroblasts
GLUT1	Glucose transporter 1
IPTG	Isopropyl β- d-1-thiogalactopyranoside
USRCAT	using Ultrafast Shape Recognition with CREDO Atom Types
PCR	Polymerase chain reaction
HBD	Hydrogen bond donor
HBA	Hydrogen bond acceptor
MTase	Methyltransferase
ATP	Adenosine Triphosphate
SBDD	Structure-based drug design
LBDD	ligand-based drug design

LIST OF SYMBOLS

%	Percentage
°F	Fahrenheit
Kb	Kilobase pair
kDa	kilodalton
°C	Celcius
hpi	Postinfection
hr	hour
mL	Milliliter
mg	Milligram
μM	Micromolar
mM	Milimolar
EC ₅₀	Half maximal effective concentration
IC ₅₀	Half maximal inhibitory concentration
ns	Nanosecond
μl	Microliter
U	Unit
ng	Nanogram
rpm	Remote patient monitoring
K _m	Michaelis constant
V _{max}	The maximum rate of reaction
g	gram
CV	Column Volume
μg	Microgram
nm	Nanometer
S	Substrate
Å	Angstrom
M.W	Molecular Weight

CHAPTER ONE

INTRODUCTION

1.1 BACKGROUND OF THE STUDY

The world is still experiencing a steady rise in the number of dengue-related cases, in which the prevalence remains high with no specific medications. According to the World Health Organization, current studies estimated that 100-400 million dengue infections occurred every year, where 3.8 billion people are at risk of infection. (WHO, 2020). Every year, 500,000 cases developed into severe dengue disease which consequences up to 25,000 deaths annually, worldwide (WMP, 2019). At present, there are more than 129 countries that were impinged with this disease, where 70% of the burden is in Asia (WHO, 2020).

Dengue is the most pivotal emerging arboviral disease caused by four dengue virus (DENV) serotypes (DENV-1, DENV-2, DENV-3, and DENV-4) that belong to the Flaviviridae family (Wichapong et al., 2013; Malavige et al., 2018). Each of the serotypes has a distinct way to cause dengue epidemics and is associated with severe dengue. The female *Aedes aegypti* carries the virus and transmits it *via* a single bite to the human's body (Wichapong et al., 2013), where dengue infection ranged from self-limited dengue fever (DF) to life-threatening syndrome called dengue haemorrhagic fever (DHF) and dengue shock syndrome (DSS) (Diamond & Pierson, 2015). Dengue fever symptoms usually appear within four to seven days after being bitten by an infected mosquito, while the mild case of dengue fever may not show any symptoms.

Dengue is a flu-like illness that infects infants, youngsters, and adults, but only severe dengue causes death. Mild dengue symptoms are exhibited by high fever (104°F) with severe headache, pain behind the eyes, muscle and joint pains, nausea, vomiting,

and swollen glands or rash, while severe dengue symptoms are severe abdominal pain, bleeding from gums and nose, blood in urine, stool or vomit, difficulties to rapid breathing, fatigue and restlessness (Majeed et al., 2017).

The severity of the dengue disease relies on the sequential attack by the different serotypes. For example, it was shown that DENV-1 was more virulent compared to DENV-2, based on the clinical manifestation, hematological parameters, and genotypic variation of limited dengue cases (Lee et al., 2015; Fried et al., 2010). The severity of dengue fever correlates with dengue serotypes because of host immune response, where immunity does form when the person becomes infected with one type of serotype but does not apply when a secondary infection develops with another serotype; where this can lead to death (Taslim et al., 2018). At present, DENV-2 is considered the most virulent serotype, based on the clinical data and laboratory test report (Wijewickrama et al., 2018; Vinodkumar et al., 2013). However, it is still difficult to distinguish the specificity of serotypes in terms of their severity, although they share approximately 65% genomic character (Mirza et al., 2016; Lee et al., 2015).

At present, no effective vaccines or specific drugs that can be integrated into the global dengue prevention and control strategy exist (WHO, 2019). However, as a part of their recent clinical study, Godói et al. (2012) has produced the first dengue vaccine known as Dengvaxia (CYD-TDV), which was registered in Mexico by Sanofi Pasteur. At present, the vaccine cannot provide long-term protection against all four serotypes, and it is only effective for children aged 2–16 years (Godói et al., 2012). It has also been established that sequential infections with different serotypes increased the chances of developing severe disease, which limits the use of vaccination as an early step in dengue prevention. As previously noted, no well-developed and specific anti-dengue drugs presently exist. Hence, treatment mostly relies on rehydration therapy.

The limitation of rehydration therapy is that it cannot cure the severe condition. This necessitates the discovery of new potentially effective drugs that may serve as the first line of treatment for dengue fever.

Viruses are non-living entities and inherently they do not have their metabolism (Sanchez & Michale, 2017). Hence, they depend on the cellular metabolism of the host cell to supply the energy and macromolecules necessary for successful replication (Krystal et al., 2015). It has been shown that cellular metabolic changes, particularly glycolysis correlated with dengue infection in primary human cells (Krystal et al., 2015). During the event, phosphorylation of glucose is catalyzed by the first enzyme of glycolysis; hexokinase (HK), and subsequently produces pyruvate (Roberts et al., 2014). Hexokinase has four isoforms (HKI, HKII, HKIII, HKIV), where HKII is the main enzyme found in insulin-sensitive tissues such as skeletal and cardiac muscles, as well as adipose tissue (Robert et al., 2014). HKII is also the key catalytic enzyme involved in limiting the rate of glycolysis, specifically in converting glucose to glucose-6-phosphate (Wolf et al., 2011). It has been reported that during dengue infection, notable glucose consumption was observed and absorption of exogenous glucose has a great impact on dengue replication (Krystal et al., 2015). This subsequently resulted in increased expression of human HKII in the virus-infected cell compared to the mock cell, which highlighted the potential of the enzyme as an attractive drug target for anti-DENV drug development. Hence, the main focus of this research is to identify and validate potential compounds that specifically target HKII through *in silico* screening and inhibition analysis, which can further be developed as anti-dengue therapeutics.